with 6× SSPET at 22°C, and stained at room temperature with staining solution [streptavidin R-phycoerythrin (2 μg/ml) (Molecular Probes) and acetylated bovine serum albumin (0.5 mg/ml) in 6× SSPET] for 8 min. After they were stained, the chips were washed 10 times with 6× SSPET at 22°C on a fluidics workstation (Affymetrix). Hybridization to the chip was detected by using a confocal chip scanner (HP/Affymetrix) with a resolution of 40 to 80 pixels per feature and a 560-nm filter.

17. Candidate SNPs were identified by using a combination of four algorithms followed by a visual inspection. At each position, the VDA contains one "expected" probe (corresponding to the sequence from which the chip was designed) and three "variant" probes (containing a substitution in the central position). The first algorithm (base-calling) looked for positions at which, in some individuals, a variant probe gave a stronger signal than the expected probe. The second algorithm (clustering) considered the signal vector $\mathbf{s}_{ij}$ from the eight probes at position i (four base substitutions on both strands) in individual j and looked for positions i at which the vectors $\mathbf{s}_{ij}$ fell into multiple clusters. The third algorithm (mutant fraction) was similar but focused only on the expected probe and a single variant probe at a time (rather than all three variant probes). The fourth algorithm (footprint detection) looked for the loss of signal that occurs at the expected probes in the neighborhood of an SNP (*13, 15*). The algorithms have different sensitivities for detecting heterozygous and homozygous variations.
18. As discussed in the text below, the proportion K of polymorphic sites is expected to be proportional to $[1^{-1} + 2^{-1} + 3^{-1} + \ldots + (n-1)^{-1}]$, where n is the number of genomes sampled. The proportion of polymorphic sites is thus expected to increase by 39.3% when the number of genomes is increased from 6 (in the gel-based survey) to 14 (in the chip-based survey). This agrees well with the observed increase of 38.8%.
19. A relatively small sample size suffices to capture much of the common variation. The sample size of 14 has a 50% chance of detecting an allele with a frequency of 5%. Doubling the proportion of variant sites identified would require increasing the number of genomes surveyed from 14 to 325, on the basis of the formula for K. The larger sample size will tend to identify polymorphisms with lower heterozygosity.
20. STSs were resequenced on both strands with dye-primer and dye-terminator chemistry.
21. The chip-based approach has the further advantage that long STSs can be analyzed, whereas gel-based sequencing is limited to about 600 bp. It is thus possible to use fewer PCR products to analyze a region. The current study did not take advantage of this feature because we used short STSs already available from our previous work (*6, 7*).
22. Confirmation was initially performed by multipass sequencing but is currently being done by using the clustering test on genotyping chips.
23. M. A. Walter *et al.*, *Nature Genet.* **7**, 22 (1994).
24. The lowest density occurs on chromosome X, which has the lowest density of STSs and which was screened in fewer total genomes in as much as the screening panel included three males.
25. For each SNP, PCR primers were chosen with the PRIMER software package (*6*) to closely flank the polymorphic base and to have a predicted melting temperature of 57°C. Forward and reverse primers were synthesized with the T7 and T3 promoter sites (5′-TAATACGACTCACTATAGGGAGA-3′ and 5′-AATTAACCCTCACTAAAGGGAGA-3′) at their respective 5′-ends. Each PCR primer pair was individually tested to determine if it produced a single clear fragment visible by agarose gel electrophoresis and ethidium-bromide staining, as described (*6*). PCR assays passing this test were further classified as being strong or weak according to the yield of the fragment produced. Primer pairs were grouped into multiplex sets, with the sets chosen to consist of either strong assays or weak assays.
26. Multiplex PCR was performed by using multiple PCR primer pairs in a single reaction. Specifically, multiplex PCR reactions were performed in a 50-μl volume containing 100 ng of human genomic DNA, 0.1 to 0.2 μM of each primer, 1 unit of AmpliTaq Gold (Perkin-Elmer), 1 mM deoxynucleotide triphosphates (dNTPs), 10 mM tris-HCl (pH 8.3), 50 mM KCl, 5 mM $MgCl_2$, and 0.001% gelatin. Thermocycling was performed on a Tetrad (MJ Research), with initial denaturation at 96°C for 10 min followed by 30 cycles of denaturation at 96°C for 30 s, primer annealing at 55°C for 2 min, and primer extension at 65°C for 2 min. After 30 cycles, a final extension reaction was carried out at 65°C for 5 min. Because the resulting PCR products were small, it was unnecessary to fragment them (as was done for the STSs in the SNP screen). The PCR products were then labeled with biotin in a standard PCR reaction, by using T7 and T3 primers with biotin labels at their 5′-ends. The reaction was performed with 1 μl of template DNA, 0.1 to 0.2 μM labeled primer, 1 unit of AmpliTaq Gold (Perkin-Elmer), 100 μM dNTPs, 10 mM tris-HCl (pH 8.3), 50 mM KCl, 1.5 mM $MgCl_2$, and 0.001% gelatin. Thermocycling was performed with initial denaturation at 96°C for 10 min followed by 25 cycles of denaturation at 96°C for 30 s, primer annealing at 52°C for 1 min, and primer extension at 72°C for 1 min. After 25 cycles, a final extension reaction was carried out at 72°C for 5 min. The PCR products from the various multiplex reactions for an individual were then pooled together. One-tenth of the pooled sample was denatured and used for chip hybridization. Chips were hybridized, washed, stained and scanned, as above (*16*).
27. D. G. Wang, unpublished observations.
28. A classification procedure for assigning genotypes was derived for each locus on the basis of the hybridization results observed in a test population of 39 individuals. The proportions of the two alleles present in the i-th sample, denoted $\pi_{A,i}$ and $\pi_{B,i}$, (with $\pi_{A,i} + \pi_{B,i} = 1$) were estimated essentially by comparing the observed hybridization signal to the expected signals for the two VDAs. The values $\pi_{A,i}$ for the 39 individuals lie in the interval [0,1] and should ideally cluster near 0, 0.5, and 1.0, but other patterns might occur because of differences in hybridization intensity between the two alleles. The values were optimally clustered (*33*) with the MODECLUS procedure of the SAS software package (SAS Institute). A maximum of three nonoverlapping clusters was permitted, defined by points with a minimum separation of 0.12. A locus failed the cluster test if all the samples fell into a single cluster, if the samples gave rise to two clusters but neither corresponded to the heterozygous genotype (AB), or if too many samples (more than 9 of 39) fell outside the three optimal clusters. A locus passing the cluster test gave rise to either three clusters (genotypes AA, AB, BB) or two clusters (genotypes AA, AB or BB, AB).
29. Subsequent samples were genotyped according to the cluster in which the hybridization pattern fell, with no genotype being called for samples falling outside these predefined clusters.
30. W.-H. Li, *Molecular Evolution* (Sinauer, Sunderland, MA, 1997); N. Takahata and Y. Satta, *Proc. Natl. Acad. Sci. U.S.A.* **94**, 4811 (1997); M. Nei and D. Graur, in *Evolutionary Biology*, M. K. Hecht, B. Wallace, G. T. Prance, Eds. (Plenum, New York, 1984), vol. 17, pp. 73–118.
31. F. J. Ayala, *Science* **270**, 1930 (1995).
32. R. C. Lewontin, in *Evolutionary Biology*, T. H. Dobzhansky, M. K. Hecht, W. C. Steere, Eds. (Appleton-Century-Crofts, New York, 1972), vol. 6, pp. 381–398.
33. M. M. DeAngelis, D. G. Wang, T. L. Hawkins, *Nucleic Acids Res.* **23**, 4742 (1995).
34. W. L. G. Koontz and K. Fukunaga, *IEEE Trans. Comp.* **C-21**, 171 (1972).
35. We thank D. Stern for construction of chip scanners used in the project, C. Chen-Cheng for computation work related to the polymorphisms among EST sequences in GenBank, T. Hawkins for sequencing of some STSs, and D. Lockhart for helpful comments on the manuscript. Supported in part by grants from Affymetrix, Millennium Pharmaceuticals and Bristol-Meyers-Squibb (to Whitehead Institute), from the National Human Genome Research Institute [to Whitehead Institute (HG00098) and Affymetrix (HG01323)] and from the National Institute of Standards and Technology [to Affymetrix (70NANB5H1031)].

5 February 1998; accepted 31 March 1998

RasGRP, a Ras Guanyl Nucleotide–Releasing Protein with Calcium- and Diacylglycerol-Binding Motifs

Julius O. Ebinu, Drell A. Bottorff, Edmond Y. W. Chan, Stacey L. Stang, Robert J. Dunn, James C. Stone*

RasGRP, a guanyl nucleotide–releasing protein for the small guanosine triphosphatase Ras, was characterized. Besides the catalytic domain, RasGRP has an atypical pair of "EF hands" that bind calcium and a diacylglycerol (DAG)-binding domain. RasGRP activated Ras and caused transformation in fibroblasts. A DAG analog caused sustained activation of Ras-Erk signaling and changes in cell morphology. Signaling was associated with partitioning of RasGRP protein into the membrane fraction. Sustained ligand-induced signaling and membrane partitioning were absent when the DAG-binding domain was deleted. RasGRP is expressed in the nervous system, where it may couple changes in DAG and possibly calcium concentrations to Ras activation.

The cellular properties of neurons are modulated by a number of extrinsic signals, including synaptic activity, neurotrophic factors, and hormones. These signaling systems alter the intracellular concentrations of second messengers such as calcium and cyclic nucleotides, and these small molecules can regulate the activities of protein kinases (*1*). As the mechanisms linking Ras signaling to nerve function are not completely understood, we developed a cDNA cloning approach to identify proteins that enhance Ras signaling in the brain. From rat brain mRNA, we derived cDNAs that

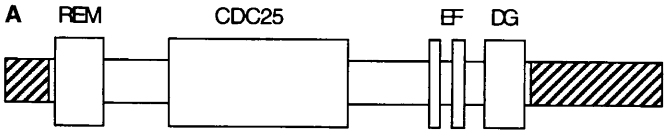

B

```
  1 MGTLGKAREAPRKPCHGSRAGPKARLEAKSTNSPLPAQPSLAQITQFRMMVSLGHLAKGASLDDLIDSCIQSFDADGNLC  80
 81 RSNQLLQVMLTMHRIIISSAELLQKLMNLYKDALEKNSPGICLKICYFVRYWITEFWIMFKMDASLTSTMEEFQDLVKAN 160
161 GEESHCHLIDTTQINSRDWSRKLTQRIKSNTSKKRKVSLLFDHLEPEELSEHLTYLEFKSFRRISFSDYQNYLVNSCVKE 240
241 NPTMERSIALCNGISQWVQLMVLSRPTPQLRAEVFIKFIHVAQKLHQLQNFNTLMAVIGGLCHSSISRLKETSSHVPHEI 320
321 NKVLGEMTELLSSCRNYDNYRRAYGECTHFKIPILGVHLKDLISLYEAMPDYLEDGKVNVQKLLALYNHINELVQLQDVA 400
401 PPLDANKDLVHLLTLSLDLYYTEDEIYELSYAREPRNHRAPPLTPSKPPVVVDWASGVSPKPDPKTISKHVQRMVDSVFK 480
481 NYDLDQDGYISQEEFEKIAASFPFSFCVMDKDREGLISRDEITAYFMRASSIYSKLGLGFPHNFQETTYLKPTFCDNCAG 560
561 FLWGVIKQGYRCKDCGMNCHKQCKDLVVFECKKRSKSPAVSTENISSVVPMSTLCPLGTKDLLHAPEEGSFIFQNGEVVD 640
641 HSEESKDRTIMLLGVSSQKISVRLKRTVAHKTTQTESFPWVGGEMPPGHFVLTSPRKSAQGALYVHSPASPCPSPALVRK 720
721 RAFVKWENKESLIKPKPELHLRLRTYQELEQEVNTLRADNDALKIQLKYAQKQIESLQLGKSNHVLAQMDHGDGT*     795
```

C

```
REM
                          *                                *    *           *    *
RasGRP     58   .KGASLDDLI DSCIQSFDAD .GNLCRSNQL LQVMLTMHRI IISSAELLQK LMNLY
RasGRF1   632   IRYASVERLL ER.......L TDLRFLSIDF LNTFLHSYRV FTDAVVVLDK LISIY
mSOS-1    617   IKAGTVLKLI ER.......L TYHMYADPNF VRTFLTTYRS FCRPQELLSL LIERF

CDC25 SCR #1
                          *    **  *
RasGRP    201   FDHL EPEELSEHLT YLEFKSFRRI
RasGRF1  1005   FENH SAMEIAEQLT LLDHLVFKSI
mSOS-1    793   LLTL HPIEIARQLT LLESDLYRAV

CDC25 SCR #2
                *                      * * *                    *   **  *
RasGRP    271   RA EVFIKFIHVA QKLHQLQNFN TLMAVIGGLC HSSISRLKET S
RasGRF1  1077   RA STIEKWVAVA DICRCLHNYN AVLEITSSIN RSAIFRLKKT W
mSOS-1    865   RV AYVSRIIEIL QVFQELNNFN GVLEVVSAMN SSPVYRLDHT F

CDC25 SCR #3
                    *  *  *        *  *
RasGRP    349   HFK IPILGVHLKD LISLYEAMPD
RasGRF1  1156   PC. VPYLGMYLTD LAFLEEGTPN
mSOS-1    942   PC. VPFFGIYLTN ILKTEEGNPE

EF-Hands
                    *  *  *  *  *****   *                            ***  * **  *   *
RasGRP    475   VDSVFKNY DLDQDGYISQEE FEKIAAS........FPF..SFCVM DKDREGLISRDE ITAYFMRA
Cal B      91   LRFAFRIY DMDKDGYISNGE LFQVLKM -[14]- VDK..TIINA DKDGDGRISFEE FCAVVGGL

DAG Domain
                * *   *   ***** *   ***  ***   * ***** *   *   *   *
RasGRP    542   HNFQETTYLK PTFCDNCAGF LWGVIKQGYR CKDCGMNCHK QCKDLVVFEC
PKCδ      231   HRFKVHNYMS PTFCDHCGSL LWGLVKQGLK CEDCGMNVHH KCREKVANLC
```

Fig. 1. Structures of rbc7 and RasGRP proteins. (**A**) Schematic domain structure map of RasGRP/rbc7. The REM box, CDC25 box, EF hands, and DAG-binding domain (DG) are shown as open boxes. The regions found in RasGRP but missing in rbc7 are shown as hatched boxes. (**B**) The sequence of RasGRP was deduced from the sequence of the rbc7 isolate and from overlapping cDNA clones. The entire coding sequence was confirmed from PCR products recovered by reverse transcription PCR from rat brain RNA. RasGRP and rbc7 differ at two internal sites: Asp[404] is Asn in rbc7 and Gly[576] is Glu in rbc7. The Met and Pro residues underlined represent the first and last residues of the deduced rbc7 product. rbc7 encodes a 550-residue, 63.4-kD product. RasGRP encodes a 795-residue, 90.3-kD product (Genbank accession number AF060819). (**C**) Sequence comparisons of the deduced protein primary structures. The REM box and the three structurally conserved regions (SCRs) within the CDC25 box (*29*) are aligned with the corresponding regions of mouse SOS1 (*10*) and rat RasGRF1 (*8*). The EF hands are aligned with those of calcineurin B (Cal B) (*30*). The DAG-binding domain of RasGRP is aligned with that of PKCδ (*31*). In all alignments, residues that are identical or chemically similar are in bold; those that are identical are marked with an asterisk. In the alignments of the REM and CDC25 boxes, residues that are underlined in RasGRP are identical or similar to either SOS1 or RasGRF1. In the alignment of the EF hands, the underlined residues are those that interact with calcium. In the alignment of the DAG domain of RasGRP to that of PKCδ, the underlined residues are those that coordinate with zinc atoms and are conserved in all DAG-binding proteins (*32*).

could complement a transformation-defective allele of v-*H-ras* in a fibroblast transformation assay 2).

One cloned cDNA, rbc7 (rat brain cDNA 7), was weakly transforming in rat2 fibroblasts in the absence of the transformation-defective allele of v-*H-ras*. However, the rbc7 product did appear to function in the Ras pathway. The morphology of transformed foci was similar to that obtained with an activated version of *Ras*. Compared with control cells, pooled populations of rbc7-expressing cells exhibited a higher saturation density, some anchorage-independent growth, and a tumorigenic phenotype. More pronounced morphological transformation was exhibited by rat2 cells expressing rbc7 and overexpressing c-*H-ras*. We also observed strong morphological transformation when rbc7 was expressed in rv68BUR, a somatic mutant that is hypersensitive to transformation by Ras. This rat2 derivative is heterozygous for an activating mutation in *Mek1*, a kinase that functions downstream of Ras in cell transformation (3, 4).

Analysis of the sequence of rbc7 and the deduced protein product indicated that the cDNA is a 5′ and 3′ truncated version of a larger normal transcript (Fig. 1A). The sequence of the normal version of rbc7, which we refer to as RasGRP (Ras guanyl-releasing protein), was determined from rat brain cDNAs isolated from a phage library and from polymerase chain reaction (PCR) products (5). Within the predicted rbc7 and RasGRP polypeptides, we identified several putative functional

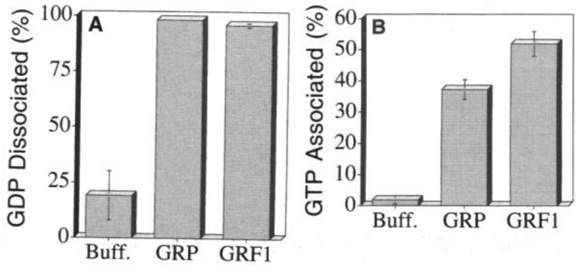

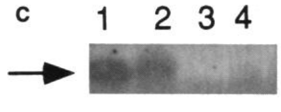

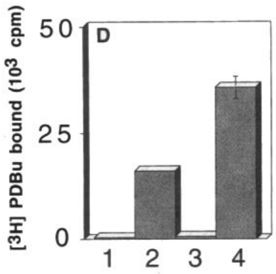

Fig. 2. Biochemical analysis of RasGRP proteins. (**A**) Dissociation of Ras-GDP promoted by RasGRP. Release of [^{3}H]GDP from Ras was followed with an immunoprecipitation procedure (*13*). Reactions included buffer (Buff.), RasGRP (catalytic region) (GRP), or p30GRF1 (GRF1), as indicated. Values represent the proportion of GDP that was released from the Ras-GDP complex and are the average of three determinations with the standard error of the mean indicated. (**B**) Association of Ras and GTP promoted by RasGRP. Ras was incubated with [α^{32}-P]GTP, and the formation of Ras-GTP was monitored (*13*). Reactions included buffer, RasGRP (catalytic region), or p30GRF1, as indicated. The amount of complex that formed is expressed as a proportion of that observed under saturating conditions. (**C**) Binding of calcium by GST-RasGRP proteins. Proteins consisting of the rbc7HA product fused to GST were resolved by SDS-PAGE, blotted to nitrocellulose, and then probed with ^{45}Ca. Lane 1, wild type; lane 2, GST-EF1$^-$ (the first EF hand mutated); lane 3, GST-EF2$^-$ (the second EF hand mutated); and lane 4, GST-EF1$^-$EF2$^-$ (both EF hands mutated) (*16*). (**D**) Interaction of the DAG-binding domain with a DAG analog. Test samples were incubated with labeled PDBu, and ligand complexed with protein was assessed by filter binding. Column 1, buffer control; column 2, 50 μg of soluble mouse brain protein (including PKC); column 3, 50 μg of GST protein; and column 4, 50 μg of GST-DG protein (*17*). Values are the average of three determinations with the standard error of the mean indicated.

J. O. Ebinu, D. A. Bottorff, E. Y. W. Chan, S. L. Stang, J. C. Stone, Department of Biochemistry, University of Alberta, Edmonton, Alberta, Canada T6G 2H7.
R. J. Dunn, Center for Research in Neuroscience, Montreal General Hospital Research Institute, Montreal, Quebec, Canada H3G 1A4.

*To whom correspondence should be addressed. E-mail: jim.stone@ualberta.ca

regions (Fig. 1). The catalytic region includes the CDC25 box, named for the prototypic Ras activator from *Saccharomyces cerevisiae* (6), and the Ras exchange motif (REM) typical of guanyl nucleotide–releasing factors that interact with Ras and its closest relatives (7). From the analysis of conserved sequences within the CDC25 box, RasGRP exhibits about 50% similarity to RasGRF1, a brain-specific Ras activator that is regulated by calcium-bound calmodulin (8, 9). RasGRP also exhibits about 50% similarity to SOS1 (10), a Ras activator that links receptor tyrosine kinases to Ras in a variety of cell types (11).

Besides the catalytic region, RasGRP has a structure resembling a pair of calcium-binding "EF hands" (12). This calcium-binding module differs from the typical paired EF hand structure in that the region between the calcium-binding loops consists of only 15 residues rather than the 20 to 30 residues typically found. RasGRP also has a diacylglycerol (DAG)–binding domain. On the basis of the sequence analysis of the CDC25 box and the presence of the EF hands and the DAG-binding domain, RasGRP appears to be a third type of mammalian Ras guanyl nucleotide–releasing factor in the CDC25 family.

We used bacterial systems to express RasGRP sequences, and the expressed proteins were tested for the relevant biochemical activities. A protein consisting of the catalytic region enhanced dissociation of the Ras–guanosine diphosphate (GDP) complex and the association of Ras with guanosine triphosphate (GTP) (Fig. 2, A and B) (13). No activity was observed when either R-Ras or RhoA was used as a substrate (14). Recombinant RasGRP protein and Ras also formed a stable complex in vitro (15). To examine binding of calcium to the EF hands, we resolved glutathione S-transferase (GST)–RasGRP fusion proteins expressed in *Escherichia coli* by electrophoresis, transferred them to a nitrocellulose filter, and probed them with ^{45}Ca (Fig. 2C). GST-GRP bound calcium, as did GST-EF1$^-$, which contains alanine substitutions in the first EF hand (16). In contrast, GST-EF2$^-$ and GST-EF1$^-$EF2$^-$, which contain substitutions in the second EF hand or both EF hands, respectively, did not bind calcium. Thus, the second EF hand is apparently the higher affinity site. A fusion protein consisting of GST and the DAG-binding domain bound to [^{3}H]phorbol 12,13-dibutyrate (PDBu), a DAG analog (Fig. 2D) (17).

To determine how the domains of RasGRP might contribute to Ras function, we engineered fibroblasts to express various forms of the protein. A hemagglutinin (HA) epitope–tagged version of the transforming sequence, rbc7HA, directed expression of a 66-kD protein (18). Relative to rat2 cells expressing the empty vector, cells expressing rbc7HA exhibited an increased amount of Ras-GTP (Fig. 3A) (19). When cells expressing rbc7HA or full-length RasGRP were treated with phorbol 12-myristate 13-acetate (PMA), a DAG analog, the amount of Ras-GTP increased. To examine the response to more physiologic stimuli, we treated cells expressing RasGRP with endothelin-1. In parental rat2 cells, this peptide growth factor results in weak activation of the mitogen-activated protein kinases, Erk1 and Erk2, probably by tyrosine kinase–dependent pathways (20). Endothelin-1 also stimulates phospholipid breakdown in rat fibroblasts (21), and this process increases the concentrations of membrane DAG and free cytoplasmic calcium. Rat2 cells engineered to express full-length RasGRP exhibited an increased level of Ras-GTP that increased further when cells were treated with endothelin-1 (Fig. 3B).

Treatment of parental rat2 cells with PMA resulted in transient and incomplete

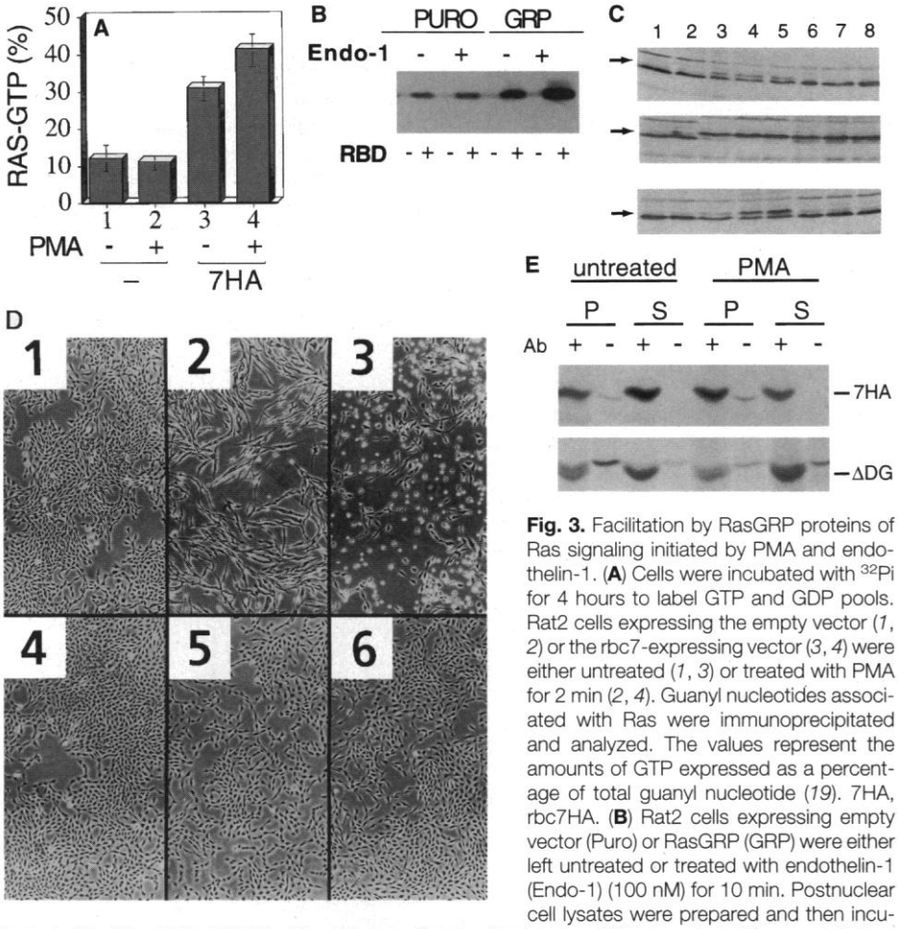

Fig. 3. Facilitation by RasGRP proteins of Ras signaling initiated by PMA and endothelin-1. (**A**) Cells were incubated with ^{32}Pi for 4 hours to label GTP and GDP pools. Rat2 cells expressing the empty vector (*1*, *2*) or the rbc7-expressing vector (*3*, *4*) were either untreated (*1*, *3*) or treated with PMA for 2 min (*2*, *4*). Guanyl nucleotides associated with Ras were immunoprecipitated and analyzed. The values represent the amounts of GTP expressed as a percentage of total guanyl nucleotide (*19*). 7HA, rbc7HA. (**B**) Rat2 cells expressing empty vector (Puro) or RasGRP (GRP) were either left untreated or treated with endothelin-1 (Endo-1) (100 nM) for 10 min. Postnuclear cell lysates were prepared and then incubated with either GST-RBD (the Ras-binding domain of Raf) (+) or GST alone (–). After precipitation, 21-kD Ras was detected with an immunoblot method. Cells also overexpressed c-H-Ras. The total amounts of Ras in the lysates were very similar. (**C**) The activation state of Erk was assessed with an SDS-PAGE mobility shift assay after various periods of PMA treatment. Lanes 1 to 8, untreated or treated for 2, 5, 10, or 60 min or 4, 6, or 8 hours. Rat2 cells expressed empty vector (top), rbc7HA (middle), or ΔDG (bottom). The arrows indicate the positions of the phosphorylated pp42 species of Erk2. Erk1 behaved similarly but was only visualized upon longer exposure to film. (**D**) Cell morphology was studied after exposure to PMA (100 nM) for 40 hours. Rat2 cells expressing rbc7HA were exposed to solvent control (panel 1), PMA (10% serum) (panel 2), or PMA (0.5% serum) (panel 3). Rat2 cells expressing ΔDG were exposed to solvent control (panel 4), PMA (10% serum) (panel 5), or PMA (0.5% serum) (panel 6). (**E**) Rat2 cells that expressed either rbc7HA or ΔDG were labeled with [^{35}S]methionine overnight, treated with either solvent or PMA for 2 min, and then disrupted in a Tenbroeck-style homogenizer. After a low-speed centrifugation to remove unbroken cells and nuclei, the lysates were centrifuged at 100,000*g* to prepare particulate (P) and soluble (S) fractions. Proteins in each fraction were solubilized in buffer containing Triton X-100, and RasGRP proteins were precipitated with an antibody to HA, resolved by SDS-PAGE, and visualized by fluorography.

activation of Erk (Fig. 3C). This process may have involved the direct activation of the Raf-Mek-Erk protein kinase cascade by protein kinase C (PKC) (*22*), and it did not involve an increase in Ras-GTP (Fig. 3A). When cells expressed full-length RasGRP or the truncated rbc7HA protein, PMA-induced activation of Erk was strong and sustained. When cells expressed ΔDG, a version of rbc7HA missing the DAG-binding domain (Fig. 1A), Erk activation was similar to that seen with the empty vector (Fig. 3C).

When subjected to prolonged exposure to PMA, rat2 cells expressing rbc7HA assumed a transformed morphology (Fig. 3D). Reducing the concentration of serum in the culture medium from 10 to 0.5% exaggerated this effect of PMA on morphology, although serum reduction alone was without effect. The ΔDG protein did not facilitate a substantial PMA-induced change in cell morphology, confirming the importance of the DAG-binding domain for RasGRP signaling.

To question whether DAG signaling might serve to recruit RasGRP to the plasma membrane, where it can interact efficiently with Ras, we monitored subcellular fractionation of RasGRP. Less than half of the rbc7HA protein was found in the membrane preparation from untreated cells. More of the protein was associated with the membrane fraction after PMA treatment (Fig. 3E). This increase was not seen with the ΔDG protein.

A single 5.6-kb RasGRP RNA species was detected in brain but not in other tissues (Fig. 4A) (*23*). Expression of the normal RasGRP transcript was widespread in the brain with the highest grain densities in the hippocampal CA1 and CA3 fields (Fig. 4B) (*24*). The majority of the grains were located within the pyramidal cell layers, probably over the pyramidal cell bodies. In contrast, we did not detect RasGRP mRNA in the granule cells of the adjacent dentate gyrus.

Ras-GTP is thought to stimulate at least two effector pathways: the Raf-Mek-Erk kinase cascade and the phosphoinositide 3-OH kinase pathway, which can result in activation of the protein kinase Akt/PKB (*25*). In neurons, signaling in the Raf-Mek-Erk pathway promotes differentiation, axonal growth, and synaptic plasticity (*26*), whereas signaling through Akt/PKB is associated with cell survival (*27*). Our characterization of RasGRP suggests that it is a Ras activator that links DAG and possibly calcium second messengers to Ras output in neurons. Both calcium and DAG can arise from several sources in neurons, and they could affect RasGRP independently. Alternatively, receptors linked to phospholipase C stimulate cleavage of phosphatidylinositol bisphosphate, and the resulting calcium and DAG signals could coordinately regulate RasGRP (*28*).

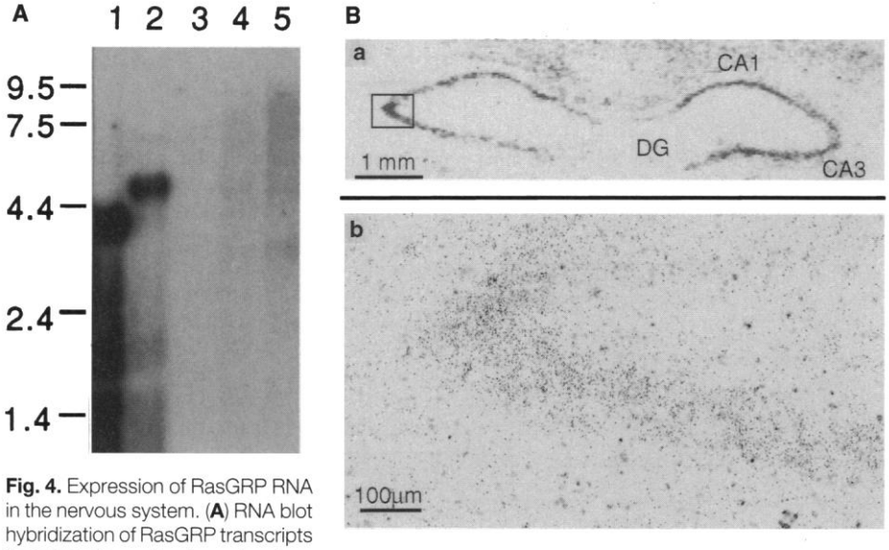

Fig. 4. Expression of RasGRP RNA in the nervous system. (**A**) RNA blot hybridization of RasGRP transcripts from transformed cells and various adult rat tissues. Lane 1, rat2 cells engineered to express rbc7HA; lane 2, brain; lane 3, liver; lane 4, lung; and lane 5, intestine. In other blots, heart, muscle, spleen, and uninfected rat2 fibroblasts were negative. Exposure was for 4 days. The agarose gel was stained with ethidium bromide before blot transfer to check that the RNA was intact and that each lane contained similar amounts of RNA. Numbers at left are molecular masses given in kilobases. (**B**) Expression of RasGRP mRNA in the adult hippocampus. (**a**) Film autoradiograph of coronal section showing localization of RasGRP mRNA in CA1 and CA3. Label in the dentate gyrus (DG) is not above background levels. (**b**) Emulsion autoradiography showing the section outlined by the square in (a). RasGRP is restricted to the regions over the pyramidal cell bodies in these sections.

REFERENCES AND NOTES

1. A. Ghosh and M. E. Greenberg, *Science* **268**, 239 (1995).
2. RNA was isolated from the brain of an adult Sprague Dawley rat by the Trizol method (Gibco BRL), and polyadenylate RNA was selected with the Fasttrack system (Invitrogen). Synthesis of cDNAs was achieved with a combination of oligo(dT) and random DNA primers (Invitrogen). DNAs were cloned with Bst X1 adapters into the retrovirus vector pCVT1B [I. Whitehead, H. Kirk, R. Kay, *Mol. Cell. Biol.* **15**, 704 (1995)]. After amplification of the library in *E. coli*, purified plasmids were converted to retrovirus form with a high-efficiency packaging system [W. Pear *et al.*, *Proc. Natl. Acad. Sci. U.S.A.* **90**, 8392 (1993)]. To create a host cell line that was sensitive to weak transforming signals in the Ras pathway, we first engineered rat2 fibroblasts to express the v-*H-ras* Y32R ($Tyr^{32} \rightarrow$ Arg substitution) effector mutant using a helper-free, *tk* retrovirus vector (*3*). This mutation in v-*H-ras* is transformation-defective in rat2 cells, but it does transform the somatic mutant rv68BUR and has been used to select extragenic suppresser mutations in *Mek1* (*4*). The encoded Ras protein interacts weakly with Raf in the yeast two-hybrid system [S. Stang *et al.*, *Mol. Cell. Biol.* **17**, 3047 (1997)]. Superinfection of Y32R-expressing rat2 cells with the viruses representing the cDNA library resulted in rare transformed foci. DNA extracted from focus-derived cell lines was used as a template in a PCR protocol, and recovered DNA fragments were cloned into pCTV3B, which expresses the selectable marker *hygro*. Individual plasmids were converted to virus form and tested for transformation. Transforming cDNAs were identified by sequence analysis.
3. J. C. Stone and R. Blanchard, *Mol. Cell. Biol.* **11**, 6158 (1991).
4. D. Bottorff, S. Stang, S. Agellon, J. C. Stone, *ibid.* **15**, 5113 (1995).
5. A rat brain cDNA library in a phage vector was screened with an rbc7 probe, and overlapping cDNA inserts representing the 5′ and 3′ ends of RasGRP were recovered. These inserts were sequenced to identify an in-frame initiator methionine preceded by a Kozak consensus sequence and the first downstream, in-frame stop codon. The entire sequence of RasGRP was verified by sequence analysis of a DNA fragment recovered from rat brain RNA with a reverse transcription PCR (Fig. 1).
6. D. Broek *et al.*, *Cell* **48**, 789 (1987).
7. C.-C. Lai, M. Boguski, D. Broek, S. Powers, *Mol. Cell. Biol.* **13**, 1345 (1993).
8. C. Shou, C. L. Farnsworth, B. G. Neel, L. A. Feig, *Nature* **358**, 351 (1992).
9. C. L. Farnsworth *et al.*, *ibid.* **376**, 524 (1995).
10. P. Chardin *et al.*, *Science* **260**, 1338 (1993); D. Bowtell, P. Fu, M. Simon, P. Senior, *Proc. Natl. Acad. Sci. U.S.A.* **89**, 6511 (1992).
11. S. E. Egan and R. A. Weinberg, *Nature* **365**, 781 (1993).
12. N. C. J. Strynadka and M. N. G. James, *Annu. Rev. Biochem.* **58**, 951 (1989).
13. Wild-type H-Ras and the p30 catalytic domain of RasGRF1 [L. Leonardsen, J. E. DeClue, H. Lybaek, D. R. Lowy, B. M. Willumsen, *Oncogene* **13**, 2177 (1996)] were expressed with His tags in Sf9 cells with the use of baculovirus vectors. The 51-kD RasGRP catalytic region (His^6 fused to RasGRP residues 49 to 471) was expressed with the pET21a vector in *E. coli*. All three proteins were purified by nickel chromatography and dialyzed into buffer A [20 mM tris (pH 7.5), 100 mM NaCl, 1.0 mM $MgCl_2$, 1.0 mM dithiothreitol, and 10% glycerol]. To follow GDP release, we incubated 1.0 μg of Ras complexed with [^{3}H]GDP (33.5 Ci/mmol) in the presence of 100 uM unlabeled GTP plus either buffer A (negative control), 3.0 μg of RasGRP, or 0.5 μg of p30GRF1 (positive control) in 0.05 ml at 30°C. The amount of radioactivity associated with Ras after 30 min was then determined by collecting Ras-GDP on beads coated with Y13-259 antibody to Ras, followed by washing and scintillation counting. Values shown in Fig. 2A are the amount of radioactivity dissociated ex-

pressed as a percentage of that associated with Ras when the 30°C incubation was omitted. To monitor the association of Ras with GTP directly, we incubated 1.0 μg of Ras with 1.25 nmol of [α^{32}-P]GTP (8 Ci/mmol) and either buffer A, 2.7 μg of RasGRP (catalytic region), or 0.44 μg of p30GRF1 in 0.05 ml for 10 min at 30°C. Complexes were recovered as above. The values in this case are expressed in Fig. 2B as the percentage of maximal exchange, as observed when the control sample was adjusted to 2.0 mM EDTA and $MgCl_2$ was added to 20 mM. The values obtained with buffer represent the spontaneous dissociation-association reactions. For both guanyl nucleotide exchange assays, the results are representative of three experiments.
14. J. O. Ebinu and J. C. Stone, unpublished data.
15. E. Y. W. Chan and J. C. Stone, unpublished data.
16. *E. coli* strains were induced with isopropyl-β-D-thiogalactopyranoside to express GST-rbc7HA fusion proteins, and cells were lysed in SDS. Total cell lysates were resolved by SDS–polyacrylamide gel electrophoresis (SDS-PAGE), blotted to nitrocellulose, and probed with [^{45}Ca] as described [K. Maruyama, T. Mikawa, S. Ebashi, *J. Biochem.* **95**, 511 (1984)]. The *EF1*$^-$ allele is a quadruple substitution converting each of the calcium-binding residues 483, 485, 487, and 493 to alanine. The *EF2*$^-$ allele similarly substitutes residues 510, 512, 514, and 521 in the second EF hand. *EF1*$^-$*EF2*$^-$ contains all eight substitutions. Coomassie blue staining of a parallel gel demonstrated that equivalent amounts of fusion protein of each genotype were expressed. The experiment was duplicated.
17. [^{3}H]PDBu binding in the presence of phosphatidylserine was performed as described [Y. Tanaka, R. Miyake, U. Kikkawa, Y. Nishizuka, *J. Biochem.* **99**, 257 (1986)]. The GST-DAG protein contains residues 538 to 598 of RasGRP. Mouse brain extracts, which contain substantial amounts of PKC, were used as a positive control. The experiment was duplicated.
18. For these studies, we used a modified version of the original cDNA, rbc7HA, cloned in the retrovirus vector pBabepuro [J. P. Morgenstern and H. Land, *Nucleic Acids Res.* **18**, 3587 (1990)]. This modified sequence includes a synthetic Kozak consensus sequence and extends from the internal initiator methionine underlined in Fig. 1B to the premature stop codon. The sequence TATGATGTTCCTGATTATGCTAGCCTC was inserted immediately upstream of this stop codon. It encodes the HA ("Flu") epitope. rbc7 and rbc7HA are similar biologically.
19. Ras-GTP levels in rat2 cells and rat2 cells expressing rbc7 were compared with a ^{32}Pi-labeling method. After treatment with PMA (100 nM for 2 min), cells were lysed, and Ras-GDP and Ras-GTP were immunoprecipitated with antibody Y13-259. Ras-associated guanyl nucleotides were then separated by chromatography and quantified by phosphorimager analysis [J. C. Stone, M. Colleton, D. Bottorff, *Mol. Cell. Biol.* **13**, 7311 (1993)]. The bars in Fig. 3A represent the standard deviation of the mean of three separate experimental values. The amounts of Ras-GTP were compared in rat2 cells expressing the empty vector and rat cells expressing full-length RasGRP with a method that takes advantage of the ability of Ras-GTP to bind the Ras-binding domain of Raf [S. Taylor and D. Shalloway, *Curr. Biol.* **6**, 1621 (1996)]. Cells were treated with endothelin-1 (100 nM for 10 min) and then lysed. The amount of Ras that associated with either GST-Raf (Raf-binding domain) or GST (negative control) was determined by immunoblotting with an antibody to Ras. Lysates contained very similar amounts of Ras.
20. H. Daub, F. U. Weiss, C. Wallasch, A. Ullrich, *Nature* **379**, 557 (1996).
21. I. Ambar and M. Sokolovsky, *Eur. J. Pharmacol.* **245**, 31 (1993).
22. W. Kolch *et al.*, *Nature* **364**, 249 (1993).
23. RNA was extracted from adult rat tissues with the Trizol method. Total RNA (10 μg) was resolved by electrophoresis in 1% agarose in borate buffer, blotted onto Hybond nylon membrane (Amersham), hybridized with RasGRP cDNA probe, and washed at high stringency.
24. In situ hybridization was done on 10-μm sections of adult rat brain [D. M. Simmons *et al.*, *J. Histotechnol.* **12**, 169 (1989)]. A ^{35}S-labeled RNA probe consisting of bases 1831 to 2014 of RasGRP was used for hybridization, and the sections were dipped in NTB2 emulsion and exposed for 15 days. Control hybridizations to adjacent sections with a sense probe showed a low amount of diffuse, uniform labeling.
25. A. B. Vojtek, S. M. Hollenberg, J. A. Cooper, *Cell* **74**, 205 (1993); L. Van Aelst, M. Barr, S. Marcus, A. Polverino, M. Wigler, *Proc. Natl. Acad. Sci. U.S.A.* **90**, 6213 (1993); X. Zhang *et al.*, *Nature* **364**, 308 (1993); P. H. Warne, P. Rodriguez-Viciana, J. Downward, *ibid.*, p. 352; P. Rodriguez-Viciana *et al.*, *ibid.* **370**, 527 (1994); P. Rodriguez-Viciana *et al.*, *Cell* **89**, 527 (1997).
26. G. D. Borasio *et al.*, *Neuron* **2**, 1087 (1989); G. D. Borasio *et al.*, *J. Cell Biol.* **121**, 665 (1993); M. Lohof, N. Y. Ip, M. Poo, *Nature* **363**, 350 (1993); S. Cowley, H. Paterson, P. Kemp, C. J. Marshall, *Cell* **77**, 841 (1994); H. Kang and E. M. Schuman, *Science* **267**, 1658 (1995); C. D. Nobes, J. B. Reppas, A. Markus, A. M. Tolkovsky, *Neuroscience* **70**, 1067 (1996); H. N. Marsh and H. C. Palfrey, *J. Neurochem.* **67**, 952 (1996); K. C. Martin *et al.*, *Neuron* **18**, 899 (1997); R. Brambilla *et al.*, *Nature* **390**, 281 (1997).
27. H. Dudek *et al.*, *Science* **275**, 661 (1997).
28. M. J. Berridge, *Nature* **361**, 315 (1993).
29. M. S. Boguski and F. McCormick, *ibid.* **366**, 643 (1993).
30. A. Aitken, C. B. Klee, P. Cohen, *Eur. J. Biochem.* **139**, 663 (1984).
31. J. P. Aris *et al.*, *Biochim. Biophys. Acta* **1174**, 171 (1993).
32. Single-letter abbreviations for the amino acid residues are as follows: A, Ala; C, Cys; D, Asp; E, Glu; F, Phe; G, Gly; H, His; I, Ile; K, Lys; L, Leu; M, Met; N, Asn; P, Pro; Q, Gln; R, Arg; S, Ser; T, Thr; V, Val; W, Trp; and Y, Tyr.
33. We thank R. Kay for advice on cDNA cloning and L. Agellon, D. Brindley, N. Dower, M. James, D. Lowy, H. Ostergaard, E. Shibuya, and B. Sykes for useful discussions. Supported by grants to J.C.S. from the National Cancer Institute, Canada.

6 May 1997; accepted 2 April 1998

Mutations in the *SMAD4/DPC4* Gene in Juvenile Polyposis

James R. Howe,* Stina Roth, John C. Ringold, Robert W. Summers, Heikki J. Järvinen, Pertti Sistonen, Ian P. M. Tomlinson, Richard S. Houlston, Steve Bevan, Frank A. Mitros, Edwin M. Stone, Lauri A. Aaltonen

Familial juvenile polyposis is an autosomal dominant disease characterized by a predisposition to hamartomatous polyps and gastrointestinal cancer. Here it is shown that a subset of juvenile polyposis families carry germ line mutations in the gene *SMAD4* (also known as *DPC4*), located on chromosome 18q21.1, that encodes a critical cytoplasmic mediator in the transforming growth factor–β signaling pathway. The mutant SMAD4 proteins are predicted to be truncated at the carboxyl-terminus and lack sequences required for normal function. These results confirm an important role for *SMAD4* in the development of gastrointestinal tumors.

Familial juvenile polyposis (JP) is an autosomal dominant disease in which individuals are predisposed to hamartomatous polyps and gastrointestinal cancer. Gastrointestinal malignancy develops in 9 to 68% of JP patients (*1*). Two groups have reported that a subset of JP patients harbor mutations in the protein phosphatase gene *PTEN*, located on chromosome 10q23 (*2*). *PTEN* is somatically mutated in many human tumor types and is the gene responsible for Cowden disease and Bannayan-Ruvalcaba-Riley syndrome (*3*). Other groups have found no evidence of linkage to markers on 10q or *PTEN* mutations in JP families (*4*). These results suggest that there is genetic heterogeneity in JP families, or that JP patients previously described with 10q abnormalities may have actually been Cowden disease or Bannayan-Ruvalcaba-Riley syndrome patients (*5*).

We recently mapped a gene predisposing to JP to chromosome 18q21.1, between markers D18S1118 and D18S487 (*6*), an interval that contains the two putative tumor suppressor genes *DCC* and *SMAD4* (*7*). The high incidence of colorectal can-

J. R. Howe and J. C. Ringold, Department of Surgery, University of Iowa College of Medicine, Iowa City, IA 52242, USA.
S. Roth and L. A. Aaltonen, Department of Medical Genetics, Haartman Institute, FIN-00014, University of Helsinki, Finland.
R. W. Summers, Department of Medicine, University of Iowa College of Medicine, Iowa City, IA 52242, USA.
H. J. Järvinen, Second Department of Surgery, Helsinki University Central Hospital, Haartmaninkatu 4, 00290 Helsinki, Finland.
P. Sistonen, Finnish Red Cross Blood Transfusion Service, Kivihaantie 7, 00130 Helsinki, Finland.
I. P. M. Tomlinson, Molecular and Population Genetics Laboratory, Imperial Cancer Research Fund, 44, Lincoln's Inn Fields, London, WC2A 3PX, UK.
R. S. Houlston and S. Bevan, Section of Cancer Genetics, Institute of Cancer Research, Sutton, Surrey SM2 5NG, UK.
F. A. Mitros, Department of Pathology, University of Iowa College of Medicine, Iowa City, IA 52242, USA.
E. M. Stone, Department of Ophthalmology, University of Iowa College of Medicine, Iowa City, IA 52242, USA.

*To whom correspondences should be addressed. E-mail: james-howe@uiowa.edu